Analysis of Interference Fit Pin Joints Subjected to Bearing Bypass Loads

T. S. Ramamurthy*
Wright Research and Development Center, MLBM, Wright Patterson Air Force Base, Ohio 45433

In advanced engineering fields such as aerospace engineering, composites are finding increasing applications because of their high strength/weight ratios. Pin joints are unavoidable in complex structures. With splice joints in spars, buklheads etc., multiple pin/rivet connections are used. Accurate analyses of stresses around pins in such situations will assist the designer to a great extent. The pins are metallic and are generally stiffer than the composites. For the purpose of analysis, the composite plate is treated as an orthotropic laminate and the pin as a rigid circular disc, and a two-dimensional linear elasticity theory is used. The geometry considered is that of a rectangular plate with a single circular pin on one of the middle lines subjected to different loads uniformly distributed stresses on two opposite sides. This is representative of a pin under the classical bearing bypass loading. In this paper an analysis of this configuration accounting for the proper pin/plate interface conditions is developed. The results highlight the nonlinear behavior of such a joint with load magnitude(s). A quadratic stress criterion is applied to evaluate the critical loadings and the corresponding strength envelopes are generated. The effect of interference fit parameter on these envelopes is estimated.

Introduction

IN advanced engineering fields such as aerospace engineering, composites are finding increasing application because of their high strength/weight and/or stiffness/weight ratios. Joints are unavoidable stress risers used in practical structures. Pin joints are very commonly used in many situations. In general the pin radius and the hole radius are not matched exactly, sometimes due to intentional clearance/interference fits and mostly due to manufacturing variations/tolerances. This misfit is defined by a parameter λ which relates the hole radius a and the pin radius a_p as

$$a_p = a(1 + \lambda) \tag{1}$$

In all cases where the pin is unbonded, the pin/plate interface exhibits a partial contact or separation behavior.[1-6] When λ is nonzero, this partial contact is a nonlinear function of the loading magnitude.[4-11] In this paper this nonlinear behavior of an interference fit pin under bearing bypass loading is studied.

The importance of pin connections in composites is evident from the number of specialists meetings held[12-14] in the recent times, the number of scientific workers engaged in this field, and the prolific literature that is being published. The problem of bypass loading on the pin was analyzed by many workers.[4,15-17] The methods of analyses of pin joints may be grouped as continuum functions,[1,16] series type solutions,[2,4,5,7,15] or numerical techniques such as finite element methods.[4,6,8-11,15,17-20] The solution techniques may further be categorized as direct or inverse methods. In the direct method, the solution is sought for a specified load level. Since for a given load, the pin/plate interface conditions are a priori unknown, one of the following two procedures is followed, viz. 1) an approximate boundary condition assumption or 2) iterative solution for the satisfaction of the proper boundary condition. In the former the extent of contact between the pin and the plate is assumed to be over a semicircular arc, and the effect of the contact load is represented by a cosinusoidal radial pressure on the hole boundary[2,18,20] or equivalent radial displacement.[19] In the iterative methods, the boundary conditions are continuously modified until the convergence is obtained.[6,11,18,20] In the 1970s a new method of solving this class of problems in isotropic plates was proposed by Rao[5] and he called it the "Inverse Technique." In this method a feasible pattern of contact/separation is initially specified from physical and symmetry conditions and the magnitude of the loading is sought from the elasticity solution. This method was later extended to orthotropic materials and to finite element techniques by Rao's colleagues including the current author.[8-10] Mangalgiri et al. developed a series of type solutions for an infinite isotropic plate with a central rigid pin subjected to both pin and plate loads and showed the existence of two different separation zones. Crews and Naik[15] have developed a finite element solution by inverse technique for a bypass load in a finite plate. They have assumed a constant bypass ratio and provided for one load magnitude for a specified contact angle. In the present paper, two separation zones are independently specified. Exploiting the symmetry of the geometry and the loading only one-half of the plate need be analyzed. In the region of analysis, there will be two locations which separate the contact and separation regions. The magnitudes of the two loads on the opposite sides of the plate are treated as dependent variables of the problem. These are solved by extending the method of inverse technique of Rao et al.[8] developed for one location of transition for the case of multiple (in the present case two) transition points. We now describe this method and present some of the new results.

Problem Definition

A typical interior pin-plate region of multiple pin/rivet connection between two components under general loading could be represented by a rectangular plate with a central pin under two different loads on the plate edges (see Fig. 1a). An end pin/rivet could be represented by a rectangular plate with an eccentric pin (see Fig. 1b). The composite plate is idealized as an orthotropic laminate, and its elastic constants are evaluated using the classical lamination theory.[21] These properties are E_1, E_2, G_{12}, and ν_{12}. For extracting the essential features of the problem with economical effort, the pin is treated as rigid and

Received March 29, 1989; revision received Oct. 2, 1989. Copyright © 1989 by T.S. Ramamurthy. Published by the American Institute of Aeronautics and Astronautics, Inc. with permission.

*Associate Professor on leave from Aerospace Engineering, Indian Institute of Science, Bangalore, India; currently Resident Research Associate.

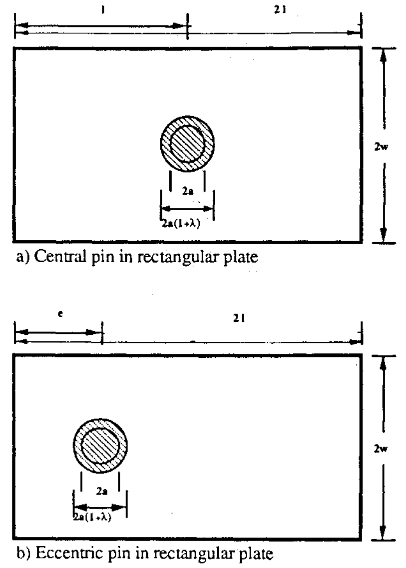

Fig. 1 Basic problem.

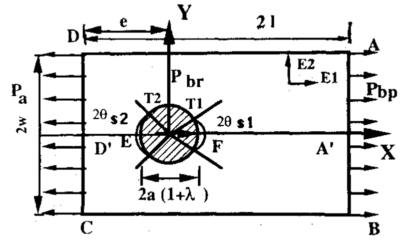

Fig. 2 Feasible plate deformation.

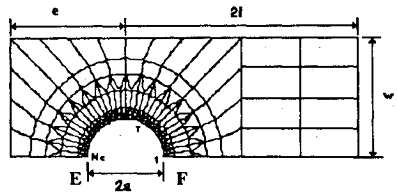

Fig. 3 Typical finite element mesh.

the pin/plate interface as perfectly smooth. It is reported in the literature that the effect of pin elasticity is negligible as compared to the effects of the pin misfit and eccentricity.[5,18]

In the present analysis, a rectangular orthotropic plate $ABCD$ of size $2w \times 2l$, of uniform thickness t, with a hole of radius a on the middle line $A'D'$ with its center at a distance e from one of the sides, for example, CD filled with a rigid pin is chosen for the study (see Fig 2). The radius of the pin is given by Eq. (1), which defines the misfit parameter λ. Depending on the value of λ, one gets various fits. A positive λ yielding interference fit, negative λ yielding clearance fit, and zero λ resulting in a neat or push fit. The origin of the coordinate system is taken at the center of the pin, and the axes are taken parallel to the orthotropic axes of the material. For simplicity the sides of the rectangle are made to coincide with the orthotropic axes. Thus the loading on the pin and the plate combination are symmetric about the X axis. Let the total load on the edge CD be P_a and on the edge, AB be P_{bp}. The difference of the two loads is the load transmitted by the pin and indicated as the pin bearing load and denoted by P_{br} resulting in the conventional bypass load problem. The gross load equilibrium condition yields

$$P_a = P_{br} + P_{bp} \tag{2}$$

A possible deformation pattern around the hole is also shown in Fig. 2 with two regions of separations $2\theta_{s1}$ and $2\theta_{s2}$ at F and E, respectively. Because of inherent symmetry in the geometry and the loading, only one half of the region, for example, $AA'D'D$ need be analyzed. In general in the region of the analysis there could be two transition points, for example, T_1 and T_2 on the hole boundary.

Method of Solution

Finite Element Formulation

As already mentioned the inverse technique proposed in the literature[8-10] is employed with the finite element solution technique for the analysis. The region of the analysis is modeled with isoparametric four noded quadrilateral and triangular elements. Since the pin is treated as rigid, only the plate is analyzed with appropriate boundary conditions at the pin/plate interface. The region around the close vicinity of the hole is divided into finer elements with a large number (Nc) of nodes on the hole boundary and element size is gradually increased by reducing the number of nodes on subsequent arcs. The region between the arcs with differing nodes is modeled by triangular elements. A typical finite element mesh is shown in Fig. 3. The nodes on the hole boundary are numbered from 1 at F to Nc at E. For ease of specifying the boundary conditions on the hole boundary, the first ring of elements are modified such that the inner node degrees of freedom are taken in the radial and tangential directions. The stiffness, displacement, and force matrices are appropriately transformed before assembling in to the global matrices, and the resulting equation may be written as

$$[K]\,[\Delta] = [F] \tag{3}$$

where $[K]$ is the global stiffness matrix, $[\Delta]$ is the nodal displacement matrix, and $[F]$ is the nodal force matrix. The solution of Eq. (3) subjected to the necessary boundary conditions yields displacement vectors and enables one to evaluate the strains and stresses at any location of interest. The necessary displacement boundary conditions are incorporated in the conventional way.[22]

Boundary Conditions

The relevant boundary conditions of the current problem may be stated as

1) for nodes on the axis of symmetry,

$$F_x = 0 \text{ and } U_y = 0$$

2) for all nodes on the hole boundary $1 < i < Nc$,

$$F_{\theta i} = 0,$$

3) $U_{ri} = a\lambda$ and $F_{ri} \geq 0$ for i in the contact region,

$$F_{ri} = 0 \text{ and } U_{ri} \geq a\lambda \text{ for } i \text{ in the separation region} \tag{4}$$

The transition nodes T_1 and T_2 are treated as part of the contact region.

Inverse Technique

As already explained, in the inverse technique, one starts with a feasible configuration and seeks the magnitude of the causative loads. This is very economical when one is developing extensive parametric data or the design information for new materials or geometric configurations. We shall now extend the procedure of the earlier inverse solutions[5,8-10] for the current problem. In the present problem, there are two transition location, T_1 and T_2. Since both locations are independently specified, there must be two independent load parameters in the problem which are to be obtained from the solution. In the present case, we select P_a and P_{bp} as two independent loadings and treat them as unknowns of the problem for a given misfit parameter λ. For convenience the following nondimensional parameters are defined,

$$\alpha = P_{bp}/(2E_1at\lambda), \qquad \beta = P_a/(2E_1at\lambda)$$

$$\gamma = P_{br}/(2E_1at\lambda)$$

$$s = (a/w)\alpha = \sigma_{bp}/(E_1\lambda), \qquad r = (a/w)$$

$$\beta = \sigma_a/(E_1\lambda) \tag{5}$$

All the deformations are normalized with $a\lambda$. In the numerical examples studied, T_1 and T_2 are made to coincide with the nodal points of the finite element idealizations. Once T_1 and T_2 are specified, all of the displacement boundary conditions in Eq. (4) are known, and the corresponding solutions are obtained for the specified loads.

Solution Procedure

Within the realm of linear elasiticity solutions, the stresses, strains, and displacements of different solutions can be added to obtain a new solution. Since the geometric configuration is not changed, the general bypass loading on the intereference fit pin in a plate is split into the following three basic loadings 1) $r = 0$, $s = 1$, and $a\lambda = 1$; 2) $r = 1$, $s = 0$, and $a\lambda = 1$; and 3) $r = 0$, $s = 0$, and $a\lambda = 1$. The finite element model is solved for the three basic load vectors represented by the three basic loadings. Since we have specified T_1 and T_2 as part of the contact zones, they satisfy the displacement conditions but not the nodal force condition. From the solution of the finite element model for the three load vectors, we get the influence coefficients for the nodal forces in the radial directions at the transition locations. They may be denoted as F_{rij} ($i = 1,2$ and $j = 1,2,3$); i refers to the transition location T_1 or T_2, and j refers to the load vector. The displacement vectors corresponding to the three load vectors may be denoted by Δ_i ($i = 1,2,3$). For the loadings of r,s, on the plate edges, the radial nodal force at the transition nodes may be written down as

$$F_{rTi} = (F_{ri1} - F_{ri3})\,s + (F_{ri2} - F_{ri3})\,r + F_{ri3}\,a\lambda \tag{6}$$

The true loading for any specified T_1 and T_2 is the set which satisfies the conditions F_{rTi} to be zero.[8,16] This yields the following set of simultaneous equations viz,

$$F_{rT1} = (F_{r11} - F_{r13})\,s + (F_{r12} - F_{r13})\,r + F_{r13}\,a\lambda = 0$$

$$F_{rT2} = (F_{r21} - F_{r23})s + (F_{r22} - F_{r23})r + F_{r23}a\lambda = 0 \tag{7}$$

The solution of Eq. (7) yields r,s, values in terms of $a\lambda$, and the final deformation vector is obtained as

$$\boldsymbol{\Delta} = s\Delta_1 + r\Delta_2 + (a\lambda - r - s)\Delta_3 \tag{8}$$

Once the displacement vector $\boldsymbol{\Delta}$ is known, the stresses and strains in the whole field may be evaluated in the conventional way.[22] For the elements on the hole edge, the stresses are transformed into the radial and tangential components and are extrapolated to the nodal point locations using the transformation matrix in the literature.[10]

Qualitative Behavior of the Joint

We shall now discuss the behavior of an interference fit joint in qualitative terms, for any specified T_1 and T_2 locations, the solution of Eq. (7) yields a set of values r,s, representing the loadings on the two edges required to sustain the configuration of transition locations at T_1 and T_2. Equation (7) represents two straight lines in the r,s, field (see Fig 4), and their intersection point is the solution set r,s. These lines represent the conditions of zero radial force at the nodes T_1, T_2. Fixing the value of T_1 and sequentially varying T_2, one gets a number of solution points, and a curve through them would represent the values of r,s, for a fixed θ_{s1} but varying θ_{s2}. Similarly by fixing T_2 and sequentially varying T_1, one gets a number of solution points, and a curve through them would represent the values for a fixed θ_{s2}. These are shown qualitatively in Fig 4. For $T_2 = Nc$, $\theta_{s2} = 0$ and $T_1 = 1$ is $\theta_{s1} = 0$. Since the configurations with either $T_1 = 1$ or $T_2 = Nc$ makes the transition locations interior points, the configurations can have nonzero force but must be compressive in nature. This is highlighted for the case $T_2 = Nc$. Since T_2 is now an interior point, only F_{rT1} need be zero, but F_{rT2} must be greater than or equal to zero. So the acceptable solutions of r,s, must lie on the line representing the condition $F_{rT1} = 0$ and yielding positive values for F_{rT2}.

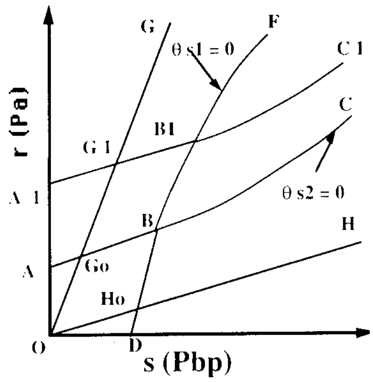

Fig. 4 Behavior of interference fit pin joint: schematic.

For the case $T_1 = 1$ and $T_2 = Nc$, the two lines of Eq. (7) yield the boundary of the region of loading for which full contact is maintained. This is shown as the quadrilateral $OABD$ in Fig 4. Fixing T_1 at 1 and varying T_2 yields a set of points through which a curve BF is drawn representing zero θ_{s1}. In the region between the curve DBF and r axis θ_{s1} will always be zero. Consider a point B_1 on the curve DBF representing some separation angle θ_{s2}. For this configuration the condition $F_{rT2} = 0$ results in the line B_1A_1 where A_1 gives the value of r for zero s. A constant θ_{s2} line above DBF will be curved line B_1C_1. Similarly for $\theta_{s2} = 0$, one gets the curve ABC. In the region of loading between the s axis and ABC, θ_{s2} is always zero. For the loadings in the region CBF, it will result in two separation regions. By generating a number of solutions for different combinations of T_1 and T_2, locations contours of constant separation angles can be drawn resulting in a nonlinear grid system.

The behavior of an interference fit pin joint under specified bypass load ratio can now be studied very easily. Let the bypass load ratio k be defined as

$$k = s/r = P_{bp}/P_a \tag{9}$$

Thus with the increase in magnitude of P_a, we get a straight line with a specified slope in Fig 4. Leg OG be one such line intersecting DB at G_0 and D_1B_1 at G_1 etc. When the loading situation is such it is within OG_0, there will be full contact. When P_a further increases to G_1, there is contact at F, but there is separation at E corresponding to the contour value of A_1B_1. Similarly if P_a is smaller than P_{bp}, we get the line OH along which θ_{s2} is zero, and θ_{s1} grows with the load beyond OH_0. If P_a and P_{bp} are such that the point lies in the region CBF, one can read or interpolate values from the grid values.

So from a given geometry and material, a graph similar to that of Fig. 4 is obtained, and the configuration for any load combination can be easily interpolated. Once P_a and P_{bp} and T_1 and T_2 locations are known, the pin bearing load can be obtained easily from the overall equilibrium condition as

$$P_{br} = P_a - P_{bp} \tag{10}$$

One can then obtain a complete stress and deformation pattern. The negative P_{br} in Eq. (10) implies reversal in the direction of the pin load direction.

Numerical Studies

The material properties used in numerical examples are given in Table 1. The numerical values of material 1 are taken from Ref. 17, the values of material 2 are taken from Ref. 8, and those of material 3 are taken from Ref 23. Material 3 is a unidirectional lamina of graphite epoxy (T300/N5208). The material strength properties for material 3 given in Table 2 are taken from Ref. 23. To check the numerical accuracy of the present method, the results of Ref. 8 are reproduced in terms of the plate stress for the initiation of separation for the interference fit pin, and obtain the nondimensional loud parameter as .17769 as against .1788 in Ref. 8. The agreement is good; the deviation is less than 1%. The reason for this could be attributed to the differences in the finite element modeling. Also the square plate studied by Eriksson[17] (material 2, $w = 12$, $a = 3$, and $\lambda = -0.01$) is analyzed with 97 nodes on the hole, and the results of the pin load reacted at one edge with a specified misfit is evaluated for different contact angles. The nondimensional variation with different separation angles is presented in Fig. 5. In Fig. 5 the positive and negative regions of the curve represent the interference fit and clearance fit of the same magnitude of λ. It is seen that the two regions are mutually exclusive. The information in this figure is replotted in Fig. 6 in a modified form. The reciprocal of the load parameter is used in Fig. 6. It is seen that the two branches of the curve combine smoothly. The intersection of the curve with the horizontal axis may be referred to as push fit angle θ_p signifying zero misfit. Thus for the push fit pin joint the angle of separation is independent of the load magnitude and is a linear problem. This confirms the findings of Noble and Hussain.[1] Our technique gives a method of estimating the push fit angle for any material and geometry. The analysis of the square plate example of Eriksson yields the pin bearing load of 11.04 kN for T_2 equal to node 45 and 7.15 kN for T_2 equals node 44. For these cases the normalized stresses are shown in Fig. 7 along with those from Ref. 17. The results of Eriksson[17] are for loads of 12 kN and 6 kN, respectively. It seen that the semicontact angles for these two cases are 73 and 78.4 deg, respectively. The corresponding contact angles derived from our result of Fig. 6 are 77.54 and 81.3 deg, respectively. The contact angles of Eriksson is obtained by iteration and the values are approximate and dependent on the mesh size. Figure 7 also shows that the maximum radial stress obtained in our results and that given by Eriksson are of the same order. The variation of the hoop stress around the hole is shown in Fig. 8. It is seen that the maximum hoop stress occurs in the region of transition from contact to separation. Also on the hole edge away from the pin bearing location, the hoop stress changes sign and becomes compressive. The method is next applied to the problem of the rectangular plate with an eccentric pin and a square plate with a central pin. The rectangular plate is made of material 2, and the square plate is made of material 1. For these examples the loadings for the various configurations are plotted in Figs. 9 and 10. These quantitative figures confirm that for the major region of loadings of bypass nature, one finds a single region of separation resulting in one transition point.

Table 1 Elastic properties used in the numerical examples

Mat. No.	E_x GPa	E_y GPa	G_{xy} GPa	ν_{xy}
1[17]	24.2	102.0	11.2	0.1044
2[8]	276.1	55.32	32.89	0.2278
3[23a]	181.0	10.3	7.17	0.28

[a]Properties refer to basic lamina.

Table 2 Strength properties of material Carbon Fiber Reinforced Plastic T300/N5208

X MPa	X' MPa	Y MPa	Y' MPa	S MPa
1500	1500	40	246	68

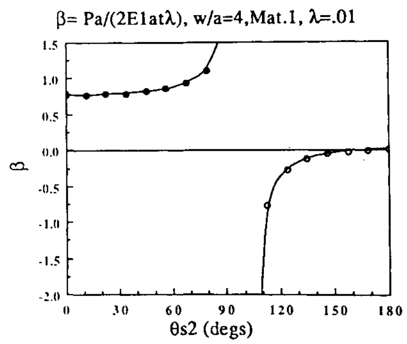

Fig. 5 Angle of separation vs β.

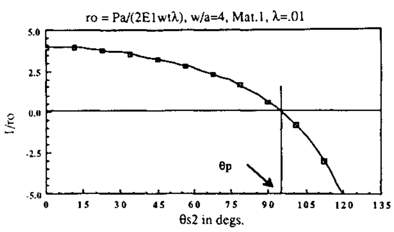

Fig. 6 Angle of separation vs $1/r_0$.

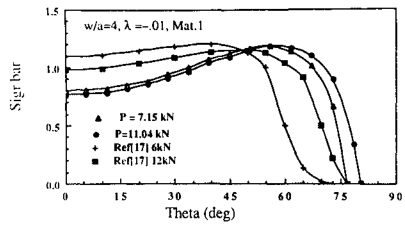

Fig. 7 Radial stress for different load levels.

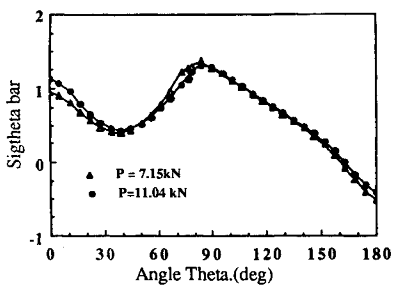

Fig. 8 Normalized hoop stress for two loads.

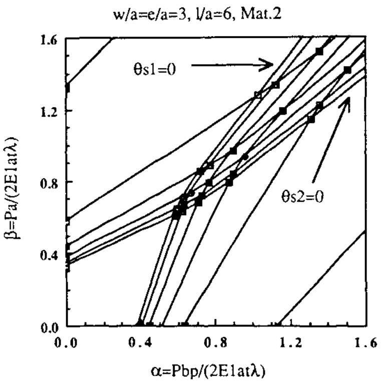

Fig. 9 Eccentric pin: α, β variation for different configurations.

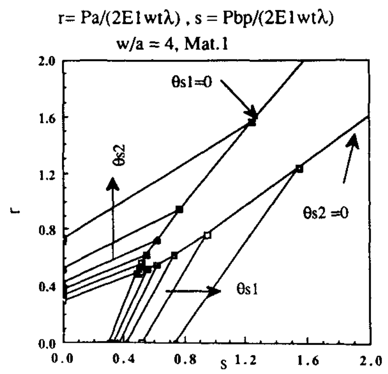

Fig. 10 Square plate central pin r, s for different configurations.

Joint Strength Evaluation

It is seen from Figs. 9 and 10 that to sustain a given configuration with one transition location the loadings on both sides of the plate have to satisfy a linear relationship of Eq. (7). So when the configuration is maintained, the internal stresses and strains can be related to external loadings by a linear equation. This aspect can be exploited to evaluate the strength of the joint by estimating the critical load for a given configuration. This is explained in the next paragraph.

Let A_1B_1 of Fig. 4 be the loading systems for a given configuration. The loading on this line satisfies the relation,

$$r = r_{0i} + D\,s \tag{11}$$

where r_{0i} and D are constants for a given configuration. Substituting this into Eq. (8) and simplifying one gets the expression for the displacement vector as

$$\Delta = \Delta_0 + \Delta_s\, s \tag{12}$$

where

$$\Delta_0 = (a\lambda - r_{0i})\,\Delta_3 \;+ r_{0i}\,\Delta_2$$

$$\Delta_s = \Delta_1 + D\Delta_2 - (1 + D)\Delta_3$$

For a given joint, once the misfit parameter λ is specified, Δ_0 and Δ_s can be evaluated, and they are constants for a given configuration. When the stresses are normalized with $E_1\lambda$ and the displacements in terms of misfit $a\lambda$, they become constants for any specified T_1, T_2. These terms do not vary with λ. So the strains evaluated from displacements of Eq. (12) will result in two components, one due to Δ_0, and the other due to Δ_s. These may be interpreted as residual strains ϵ_i^r and mechanical strains ϵ_i^m, respectively. Following the method of quadratic criterion for the maximum mechanical strains with fixed residual strains, one can obtain the critical value of s as R^m for a given location and lamina and misfit parameter. For completeness the method is briefly described below. The quadratic stress criterion is

$$F_{ij}\,\sigma_i\sigma_j + F_i\sigma_i = 1 \qquad (i = 1,2,6) \tag{13}$$

F are the strength functions of any given laminate as defined in Ref. 23. Expressing this equation in terms of strains and separating them into the residual and mechanical strains, one gets the modified equation as

$$G_{ij}\,(R^m\epsilon_i^m + R^r\,\epsilon_i^r)\,(R^m\epsilon_j^m + R^r\epsilon_j^r)$$

$$+ G_i\,(R^m\,\epsilon_i^m + R^r\,\epsilon_j^r) - 1 = 0$$

$$\epsilon_i^{\max} = R^m\epsilon_i^m + Rr\epsilon_i^r \tag{14}$$

where G_{ij} are functions of F and the laminate stiffness properties R^m is the mechanical strength ratio from which the maximum mechanical load can be computed for fixed residual load or strain; and R^r is the residual strength ratio for fixed mechanical load or strain.

Since the residual strain is evaluated for a specified λ, and we are interested in calculating the maximum mechanical load, we take $R^r = 1$ and evaluate the maximum allowable $- R^m$.

Taking $R^r = 1$, Eq. (14) can be simplified as

$$A\,(R^m)^2 + B\,R^m - 1 = 0.0 \tag{15}$$

Where A ,B are functions of ϵ^m and ϵ^r for a unit mechanical load and specified $a\lambda$. Solving Eq. (15), one obtains the value of R^m, the measure of critical mechanical load at a given location.

The strength of the joint corresponds to the least value of R^m in the whole field. This is evaluated using the method of Soni.[19] The procedure is described below. For each element around the hole, the value of R^m is evaluated independently for each ply. The least of this set corresponds to the first ply failure at that element. Since this will be highly conservative, the maximum R value for each element is considered. This would correspond to the last ply failure at an element ignoring the degradation of the element stiffness due to any failed ply.

Thus for each of the elements around the hole, a critical value of R^m is evaluated. From this set of R values, the least one is considered to be the critical value of the hole joint R^m_{cri}. This value of R yields the limiting values of r,s along A_1B_1 in Fig. 4. By repeating the process with different transition locations, one can get a contour of limiting loadings in the whole field. If one changes the value of the misfit parameter λ, the initial strains change, and hence the critical r,s values, and a new critical loading limit is obtained.

If the critical loading set (r,s) corresponding to R^m_{cri} is such that it is in the region CBF, one must solve the problem with two transitions, and the assumption of geometry invariance is violated. But the values of r,s obtained by this procedure may be taken as a first approximation. This procedure is applied to a square plate with material 3 with a central pin, and the results of critical loadings are shown in Fig. 11 for different misfit parameters. The laminate used in this example consisted of material 3 having 6, 69, 12.5, 12.5% layers in 0, 90, + 45, and − 45 deg orientations, respectively. Figure 11 shows the effect of the misfit parameter on the joint strength. The values of λ used in these results are 0.00005, 0.000025, and 0.00001. These are fractions based on Eq. (1). For low λ values approaching zero, results in the push fit joint. The limiting values for this case falls in the region CBF. So for the push fit joint with high bypass loads, the critical loading is likely to be in the two transition point region. It is seen higher; the misfit parameter value lower is the critical load boundary. This results confirm the basic concept, the higher the initial strain, the lower the mechanical loadings will be at failure. The results of Fig. 11 can be used to get critical load for any bypass

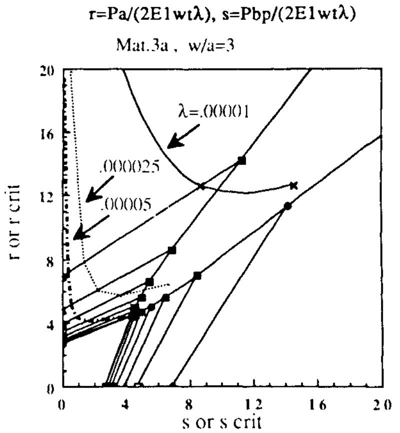

Fig. 11 Critical load envelopes for different misfits (example 1).

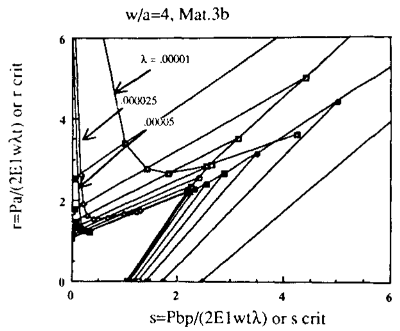

Fig. 12 Critical load envelopes for different misfits (example 2).

load ratio (value of k). Once k is specified, draw a line from the origin with the slope of k. The limiting value of r,s is at the intersection of this line with the critical load boundary. Thus this figure can be used for estimating the critical load for any specified k and used for design purposes. The same plate is analyzed with the interchange of x and y axes and referred to as material 3b, and the results are presented in Fig. 12. The strength envelopes are plotted for misfit parameters of 0.00005, 0.000025, and 0.00001.

Conclusions

A method of strength evaluation of a pin joint subjected to bypass loads accounting for proper interface conditions and consequent nonlinear behavior is successfully developed. The use of inverse technique which allows the proper specification and satisfaction of pin/plate interface conditions to solve the problem of bearing bypass loads on the pin joints is demonstrated. With minimal effort the variation of configuration for the complete range of loading is generated, and the results are economically presented. The method helps to economically generate the strength envelopes and to use them for the initial design purposes.

Acknowledgments

The author would like to acknowledge the support and encouragement from S. W. Tsai of WRDC/MLBM and the benefit of association with is colleagues A. K. Rao and B. Dattaguru at the aerostructures group at I.I.Sc., Bangalore. The author also would like to thank National Research Council USA for awarding him the Resident Research Associateship tenable at WRDC/MLBM, WPAFB, OH, during which time these studies were conducted.

References

[1]Noble, B, and Hussain, M.A., "Exact Solution of Certain Dual Series for Indentation and Inclusion Problems," *International Journal of Engineering Science,* Vol. 7, No. 11, 1969, pp. 1149-1161.

[2]De Jong, T., "Stresses Around Pin Loaded Holes in Elastically Orthotropic or Isotropic Plates," *Journal of Composite Materials*, Vol. 11, 1977, pp. 313-331.

[3]Hart-Smith, L.J., "Design Methods for Bonded/Bolted Composite Joints," Vols. 1 and 2, Airforce Wright Aeronautical Lab, Dayton, OH, AFWAL -TR-81-3154, 1981.

[4]Oplinger, D.W. and Gandhi, K.R., "Stresses in Mechanically Fastened Orthotropic Laminates," *Proceedings of the 2nd Conference on Fibrous Composites in Flight Vehicle Design*, Airforce Flight Dynamics Lab, Dayton OH, AFFDL-TR-74-103, 1974, pp. 811-842.

[5]Rao, A.K., "Elastic Analysis of Pin Joints," *Journal of Computers and Structures*, Vol. 9, 1978, pp. 125-144.

[6]Callinen, R.J., "Aeronautical Research Laboratory/Structures Rept. 439," Defense Ministry of Australia, Melbourne, Australia, AR-000-842, 1977.

[7]Hyer, M.W., Klang, E.C., and Cooper, D.E., "The Effects of Pin Elasticity, Clearance and Friction on the Stresses in a Pin Loaded Orthotropic Plate," *Journal of Composite Materials*, Vol. 21, 1987, pp. 190-206.

[8]Mangalgiri, P.D., Dattaguru, B., and Rao, A.K., "Finite Element Analysis of Moving Contact in Mechanically Fastened Joints," *Nuclear Engineering and Design*, Vol. 78, 1984, pp. 303-311.

[9]Ramamurthy, T.S., "New Studies on the Effect of Bearing Loads in Lugs with Clearance Fit Pins," *Journal of Composite Structures*, Vol. 11, 1989, pp. 135-150.

[10]Ramamurthy, T.S., "Recent Studies on the Behavior of Interfence Fit Pins in Composite Plates,"*Journal of Composite Structures*, Vol. 13, No. 2, 1989, pp. 81-99.

[11]Crews, J.H., Jr., Homg, C.S., and Raju, I.S., "Stress Concentration Factors for Finite Orthotropic Laminates with a Pin Loaded Hole," NASA TP 1862, May 1981.

[12]Kedward, K.T., ed., "*Joining of Composite Materials*," ASTM STP 749, American Society for Testing and Materials, 1981.

[13]Mathews, F.L., ed., *Proceedings of the Symposium on Joining and Repair of Fiber Reinforced Plastics*, Imperial College, Sept. 1986.

[14]"Behavior and Analysis of Mechanically Fastened Joints in Composite Structures," AGARD CP 427, 1988.

[15]Crews, J.H., Jr., and Naik, R.A., "Combined Bearing Bypass Loading on a Graphite/Epoxy Laminate," *Journal of Composite Structures*, No. 1, 1986, pp. 21-40.

[16]Mangalgiri, P.D., Ramamurthy, T.S., Dattaguru, B., and Rao, A.K., "Elastic Analysis of Pin Joints in Plates Under Some Combined Pin and Plate Loads," *International Journal of Mechanical Science*, Vol. 29, 1987, pp. 577-585.

[17]Eriksson, L.I., "Contact Stresses in Bolted Joints of Composite Laminates," *Journal of Composite Structures*, Vol. 6, No. 1, 1986, pp. 57-75.

[18]Chang, F.K., Scott, R.A., and Springer, G.S., "Failure of Composite Laminates Containing Pin Loaded Holes—Methods of Solution," *Journal of Composite Materials*, Vol. 18, 1984, pp. 225-278.

[19]Soni, S.R., "Failure Analysis of Composite Laminates with a Fastener Hole," American Society of Testing and Materials, ASTM STP 749, 1981, pp. 145-164.

[20]Tsujimoto, Y., and Wilson, D., "Elasto Plastic Failure Analysis of Composite Bolted Joints," *Journal of Composite Materials*, Vol. 20, 1986, pp. 236-252.

[21]Tasi, S. W., and Hahn, T., *Introduction to Composite Materials*, Technomic, Lancaster, PA, 1980.

[22]Zinkiewicz, O.C, *Finite Element Methods in Engineering*, 3rd ed., McGraw Hill, New York, 1977.

[23]Tsai, S. W., *Composites Design*, 3rd ed., Think Composites, Dayton, OH, 1989.